GEOPHYSICS, VOL. 71, NO. 5 (SEPTEMBER-OCTOBER 2006); P. C69–C79, 13 FIGS., 1 TABLE.
10.1190/1.2329865

Small-angle AVO response of PS-waves in tilted transversely isotropic media

Jyoti Behura[1] and Ilya Tsvankin[1]

ABSTRACT

Field records for small source-receiver offsets often contain intensive converted PS-waves that may be caused by the influence of anisotropy on either side of the reflector. Here, we study the small-angle reflection coefficients of the split converted PS_1- and PS_2-waves (R_{PS_1} and R_{PS_2}) for a horizontal interface separating two transversely isotropic (TI) media with arbitrary orientations of the symmetry axis.

The normal-incidence reflection coefficients $R_{PS_1}(0)$ and $R_{PS_2}(0)$ vanish when both half-spaces have a horizontal symmetry plane, which happens if the symmetry axis is vertical or horizontal (i.e., if the medium is VTI or HTI). For a tilted symmetry axis in either medium, however, the magnitude of the reflection coefficients can reach substantial values that exceed 0.1, even if the anisotropy strength is moderate. To study the influence exerted by the orientation of the symmetry axis and the anisotropy parameters, we develop concise weak-contrast, weak-anisotropy-approximations for the PS-wave reflection coefficients and compare them with exact numerical results. In particular, the analytic solutions show that the contributions made by the Thomsen parameters ϵ and δ and the symmetry-axis tilt ν to the coefficients $R_{PS_1}(0)$ and $R_{PS_2}(0)$ can be expressed through the first derivative of the P-wave phase velocity at normal incidence. If the symmetry-axis orientation and anisotropy parameters do not change across the interface, the normal-incidence reflection coefficients are insignificant, regardless of the strength of the velocity and density contrast. The AVO (amplitude variation with offset) gradients of the PS-waves are influenced primarily by the anisotropy of the incidence medium that causes shear-wave splitting and determines the partitioning of energy between the PS_1 and PS_2 modes.

Because of their substantial amplitude, small-angle PS reflections in TI media contain valuable information for anisotropic AVO inversion of multicomponent data. Our analytic solutions provide a foundation for linear AVO-inversion algorithms and can be used to guide nonlinear inversion that is based on the exact reflection coefficients.

INTRODUCTION

In many case studies, significant converted PS-wave energy has been observed at zero and near-zero offsets (e.g., Thomsen, 2002). In principle, this phenomenon can be explained by such factors as lateral heterogeneity and nongeometric wave propagation (Tsvankin, 1995). However, neither of those factors can account for normal-incidence far-field PS reflections in layer-cake subsurface models. Another possible reason for prominent P-to-S conversion at small offsets is the presence of velocity anisotropy above or below the reflector.

In this paper, we study the influence of anisotropy on the small-angle reflected PS-wave that generally splits into two modes traveling with different velocities — PS_1 and PS_2. The main focus of the paper is on the normal-incidence PS-wave reflection coefficients that vanish only when the reflector coincides with a symmetry plane in both half-spaces. We restrict ourselves to the most commonly used type of anisotropy — transverse isotropy (TI) with an arbitrary orientation of the symmetry axis. If the reflector is horizontal, generation of converted energy at vertical incidence requires the symmetry axis in at least one of the TI half-spaces to deviate from both the vertical and horizontal directions (i.e., the medium cannot have up-down symmetry).

Approximate weak-contrast reflection and transmission coefficients for isotropic media can be found, for example, in Aki and Ri-

Manuscript received by the Editor September 20, 2005; revised manuscript received January 11, 2006; published online September 5, 2006; corrected version published online September 20, 2006.
[1]Colorado School of Mines, Center for Wave Phenomena, Department of Geophysics, 1500 Illinois Street, Golden, Colorado 80401. E-mail: jbehura@dix.mines.edu; ilya@dix.mines.edu.

chards (2002) and Shuey (1985). Banik (1987), Thomsen (1993), and Rüger (1996, 1998, 2001) developed approximate P-wave reflection coefficients for VTI and HTI media. Rüger's results also can be applied in the symmetry planes of orthorhombic media. Pšenčík and Vavryčuk (1998) and Vavryčuk and Pšenčík (1998) presented weak-contrast, weak-anisotropy P-wave reflection and transmission coefficients for arbitrary anisotropic symmetries.

Closed-form solutions for the reflection coefficients of PS-waves in isotropic media were given by Donati (1998), Larsen et al. (1999), Alvarez et al. (1999), and Nefedkina and Buzlukov (1999). Rüger (1996, 2001) derived approximate PS-wave reflection coefficients for VTI media and for the symmetry planes of HTI media. However, as mentioned above, the normal-incidence reflection coefficients of mode conversions vanish for vertical and horizontal transverse isotropy because both models are characterized by up-down symmetry.

Weak-contrast, weak-anisotropy approximations for PS-wave reflection and transmission coefficients were extended to arbitrary anisotropy by Vavryčuk (1999), Jílek (2002a), and Artola et al. (2005). Jílek (2002b) also developed algorithms for joint inversion of PP- and PS-wave reflection coefficients in azimuthally anisotropic media. Vavryčuk (1999) and Jílek (2002b) pointed out that normal-incidence PS-wave reflection coefficients do not vanish if there is a jump in the stiffnesses c_{34} and/or c_{35} across the reflector. Artola et al. (2005) discussed the presence of normal-incidence PS-wave energy in synthetic seismograms computed for azimuthally anisotropic models.

Here, we show that the tilt of the symmetry axis in TI media can create fairly strong normal-incidence PS reflections from horizontal interfaces. (This tilt also makes the time delays of split PS-waves azimuthally dependent, and this was exploited by Angerer et al. (2002) in their characterization of dipping fractures.) Such tilted transversely isotropic (TTI) models describe dipping shale layers in fold-and-thrust belts (e.g., the Canadian Foothills) and near salt domes, dipping fracture sets, and progradational sequences. Application of the weak-contrast, weak-anisotropy approximation helps us to identify the parameter combinations responsible for the normal-incidence reflection coefficients and AVO gradients of PS-waves. We also compute the exact reflection coefficients to assess the accuracy of the linearized solutions and confirm the substantial magnitude of the small-angle PS-wave reflectivity for a range of TTI models.

ANALYTIC BACKGROUND

We start by setting up the system of linear equations that can be used to compute the exact reflection/transmission coefficients from the boundary conditions. The approximate (linearized) reflection/transmission coefficients are then obtained by applying the first-order perturbation theory.

Exact solution of the reflection/transmission problem

The reflection/transmission problem for an incident plane wave is solved by satisfying the boundary conditions at the reflector. For a welded contact of the two half-spaces, these boundary conditions are the continuity of traction and displacement, which can be written in the following compact form (e.g., Vavryčuk and Pšenčík, 1998):

$$\mathbf{C} \cdot \mathbf{U} = \mathbf{B}, \tag{1}$$

where $\mathbf{C}$ corresponds to the displacement-stress matrix for the reflected and transmitted waves, $\mathbf{B}$ is the displacement-stress vector of the incident wave, and $\mathbf{U}$ is the vector of the reflection R and transmission T coefficients of the waves P, S_1, and S_2:

$$\mathbf{C} = \begin{bmatrix} g_1^{(1)} & g_1^{(2)} & g_1^{(3)} & -g_1^{(4)} & -g_1^{(5)} & -g_1^{(6)} \\ g_2^{(1)} & g_2^{(2)} & g_2^{(3)} & -g_2^{(4)} & -g_2^{(5)} & -g_2^{(6)} \\ g_3^{(1)} & g_3^{(2)} & g_3^{(3)} & -g_3^{(4)} & -g_3^{(5)} & -g_3^{(6)} \\ X_1^{(1)} & X_1^{(2)} & X_1^{(3)} & -X_1^{(4)} & -X_1^{(5)} & -X_1^{(6)} \\ X_2^{(1)} & X_2^{(2)} & X_2^{(3)} & -X_2^{(4)} & -X_2^{(5)} & -X_2^{(6)} \\ X_3^{(1)} & X_3^{(2)} & X_3^{(3)} & -X_3^{(4)} & -X_3^{(5)} & -X_3^{(6)} \end{bmatrix}, \tag{2}$$

$$\mathbf{B} = -\left[g_1^{(0)},\ g_2^{(0)},\ g_3^{(0)},\ X_1^{(0)},\ X_2^{(0)},\ X_3^{(0)}\right]^{\mathbf{T}}, \tag{3}$$

$$\mathbf{U} = \left[R_{S1},\ R_{S2},\ R_P,\ T_{S1},\ T_{S2},\ T_P\right]^{\mathbf{T}}. \tag{4}$$

Here, $\mathbf{g}$ and $\mathbf{X}$ are the polarization and amplitude-normalized traction vectors, respectively, obtained by solving the Christoffel equation. The superscript denotes the reflected/transmitted modes, according to the following convention: 0 = incident wave; 1 = reflected S_1-wave; 2 = reflected S_2-wave; 3 = reflected P-wave; 4 = transmitted S_1-wave; 5 = transmitted S_2-wave; and 6 = transmitted P-wave. To compute the reflection/transmission coefficients, equation 1 can be solved numerically for $\mathbf{U}$.

Weak-contrast, weak-anisotropy approximation

The main goal of using linearized approximations here is to gain physical insight into the dependence of the reflection coefficients on the medium's parameters and incidence angle. Following the approach of Vavryčuk and Pšenčík (1998) and Jílek (2002a, 2002b), we linearize the boundary conditions by assuming a weak contrast in the elastic parameters across the interface and weak anisotropy in both half-spaces (see Appendix A). A homogeneous isotropic full space divided by a fictitious planar interface is taken as the background medium. The elastic parameters $a_{ijkl}^{(I)} = c_{ijkl}^{(I)}/\rho^{(I)}$ [density-normalized stiffness coefficients of the incidence (I = 1) and reflecting (I = 2) half-spaces] are expressed as small perturbations $\delta a_{ijkl}^{(I)}$ from the background values. The exact boundary conditions (equation 1) are then linearized in the small perturbations to find approximate PS-wave reflection coefficients.

Consider an incident P-wave traveling in the negative z-direction in the $[x,z]$-plane; the reflector coincides with the plane $z = 0$. The slowness vectors of the incident, reflected, and transmitted waves in the background medium can be written as (Figure 1):

$$\begin{aligned} \mathbf{p^{0(0)}} &= \mathbf{p^{0(6)}} = [p_1^0,\ 0,\ -p_3^{0P}], \\ \mathbf{p^{0(1)}} &= \mathbf{p^{0(2)}} = [p_1^0,\ 0,\ p_3^{0S}], \\ \mathbf{p^{0(3)}} &= [p_1^0,\ 0,\ p_3^{0P}], \\ \mathbf{p^{0(4)}} &= \mathbf{p^{0(5)}} = [p_1^0,\ 0,\ -p_3^{0S}]. \end{aligned} \tag{5}$$

The P-wave unit polarization vectors in the isotropic background are given by

$$\mathbf{g^{0(0)}} = \mathbf{g^{0(6)}} = \alpha\mathbf{p^{0(0)}},$$
$$\mathbf{g^{0(3)}} = \alpha\mathbf{p^{0(3)}}, \tag{6}$$

where α is the P-wave background velocity.

Polarization angle

The SV and SH polarization components can be obtained by projecting the S-wave polarization vector in the background onto the incidence $[x,z]$ plane and the direction orthogonal to it, respectively. For the perturbation approach to work in the presence of anisotropy, the chosen polarization vectors of the reflected shear waves in the background isotropic medium ($\mathbf{g^{0(1)}}$ and $\mathbf{g^{0(2)}}$) should be close to the actual polarizations ($\mathbf{g^{(1)}}$ and $\mathbf{g^{(2)}}$) (Jech and Pšenčík, 1989). Thus, the SV- and SH-wave polarization vectors ($\mathbf{g^{SV}}$ and $\mathbf{g^{SH}}$) in the isotropic background must be rotated by an angle Φ, called the *polarization angle*, which is defined uniquely away from singular directions (Jech and Pšenčík, 1989). Because the polarization angle is not a linear function of the perturbations δa_{ijkl} nor is it necessarily small, the contribution of Φ complicates the derivation of the analytic expressions for the PS-wave reflection coefficients.

If the polarization angle is known, the polarization vectors of the background shear waves S_1^0 and S_2^0 ($\mathbf{g^{0(1)}}$ and $\mathbf{g^{0(2)}}$) can be determined by rotating the SV- and SH-wave polarizations counterclockwise by the angle Φ in the plane perpendicular to the background slowness vector $\mathbf{p^{0(1)}}$ (Figure 1). Thus, $\mathbf{g^{0(1)}}$ and $\mathbf{g^{0(2)}}$ are given by

$$\mathbf{g^{0(1)}} = [\beta p_3^{0S}\cos\Phi,\ \sin\Phi,\ -\beta p_1^0\cos\Phi],$$
$$\mathbf{g^{0(2)}} = [-\beta p_3^{0S}\sin\Phi,\ \cos\Phi,\ \beta p_1^0\sin\Phi], \tag{7}$$

where β is the S-wave background velocity. Equation 7 shows that when the medium is isotropic or VTI and $\Phi = 0$ (Jech and Pšenčík, 1989), S_1^0 reduces to SV and S_2^0 reduces to SH. Similarly, the polarization vectors of the transmitted S-waves can be written as

$$\mathbf{g^{0(4)}} = [-\beta p_3^{0S}\cos\Psi,\ \sin\Psi,\ -\beta p_1^0\cos\Psi],$$
$$\mathbf{g^{0(5)}} = [\beta p_3^{0S}\sin\Psi,\ \cos\Psi,\ \beta p_1^0\sin\Psi], \tag{8}$$

where Ψ is the corresponding polarization angle. Because we are concerned with the reflected S-waves only, computation of Ψ is unnecessary because $\mathbf{g^{0(4)}}$ and $\mathbf{g^{0(5)}}$ are not involved in the linearized reflection coefficients (equation A-11).

If the medium is TTI, the polarization vector of the PS_1-wave lies in the plane formed by the symmetry axis and the PS_1 slowness vector (i.e., it is the PSV-wave in the coordinate system in which the symmetry axis is taken as vertical), whereas the PS_2-wave would be polarized orthogonal to that plane. (Note that PS_1 is not necessarily the fast PS mode.) Thus, in this case Φ is the angle between the background SV-wave polarization vector and the plane formed by $\mathbf{p^{0(1)}}$ and the symmetry axis of the incident TTI half-space. Using simple vector algebra and dropping the cubic and higher-order terms in $\sin\theta$, we find

$$\cos\Phi \approx \frac{1}{2g^2A}(2g^2\cos\phi_1\sin\nu_1 + 2g\cos\nu_1\sin\theta + \cos s\phi_1\sin\nu_1\sin^2\theta), \tag{9}$$

where

$$A \equiv \left[\sin^2\nu_1 + \frac{\cos\phi_1\sin 2\nu_1\sin\theta}{g} + \frac{(\cos^2\nu_1 - \sin^2\nu_1\cos^2\phi_1)\sin^2\theta}{g^2}\right]^{1/2}.$$

Here, ν_1 and ϕ_1 are the tilt (i.e., the angle with the vertical) and the azimuth, respectively, of the symmetry axis of the incidence TI half-space, and $g \equiv \alpha/\beta$. Although Φ can be computed from equation 9, its presence causes difficulties in deriving the approximate PS-wave reflection coefficients because Φ depends on the incidence angle θ in a rather complicated way. For an incident TI half-space, $\Phi = 0$ only when the symmetry axis is vertical ($\nu_1 = 0°$) or when the incidence plane coincides with the vertical-symmetry-axis plane (i.e., with the vertical plane that contains the symmetry axis). Note that the orien-

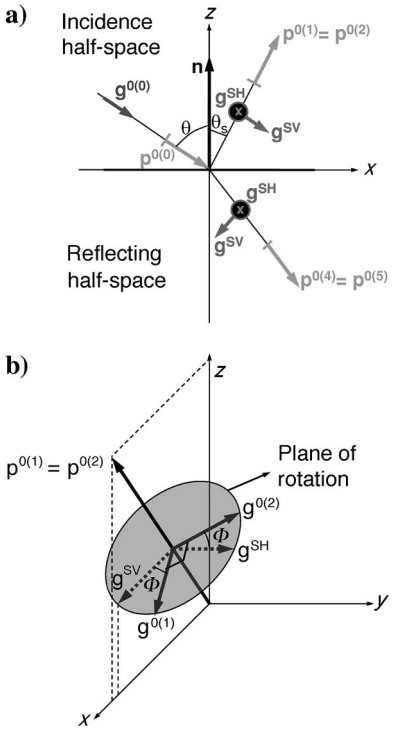

Figure 1. (a) Conventions used in solving the reflection-over-transmission problem. The incidence $[x,z]$-plane contains the interface normal $\mathbf{n}$ and the background slowness vector $\mathbf{p^{0(0)}}$ of the incident P-wave. The background S-wave slowness vectors are denoted by $\mathbf{p^{0(1)}} = \mathbf{p^{0(2)}}$ (reflected) and $\mathbf{p^{0(4)}} = \mathbf{p^{0(5)}}$ (transmitted); θ and θ_s are the phase angles of the incident P-wave and reflected S-wave. The vector $\mathbf{g}$ denotes the background polarizations. (b) Also here, $\mathbf{g^{0(1)}}$ and $\mathbf{g^{0(2)}}$ are the chosen polarization vectors of the reflected S_1- and S_2-waves, respectively, in the background medium. These vectors are obtained by rotating the background SV- and SH-wave polarizations ($\mathbf{g^{SV}}$ and $\mathbf{g^{SH}}$) by the polarization angle Φ in the plane orthogonal to the slowness vector $\mathbf{p^{0(1)}}$. If the incidence half-space is isotropic or VTI, $\Phi = 0$ (after Jílek, 2002b).

tation of the symmetry axis of the reflecting TI half-space does not influence the angle Φ.

To express the PS-wave reflection coefficient as a simple trigonometric function of θ, $\cos\Phi$ must be obtained as a polynomial of $\sin\theta$. This cannot be done, however, without assuming that $\sin^2\nu_1$ is sufficiently large, except for the special cases of normal incidence ($\theta = 0$) when Φ (equation 9) reduces to ϕ_1 and of the incidence HTI half-space ($\nu_1 = 90°$) when

$$\cos\Phi^{\mathrm{HTI}} \approx \frac{\cos\phi_1}{2g^2}(2g^2 - \sin^2\phi_1\sin^2\theta). \qquad (10)$$

Because of this problem, the linearized PS-wave reflection coefficients for oblique incidence angles are given here only if the incidence half-space is isotropic, VTI, HTI, or TTI with the symmetry axis confined to the incidence plane. For all other cases of oblique incidence of P-waves, we analyze only the exact reflection coefficients.

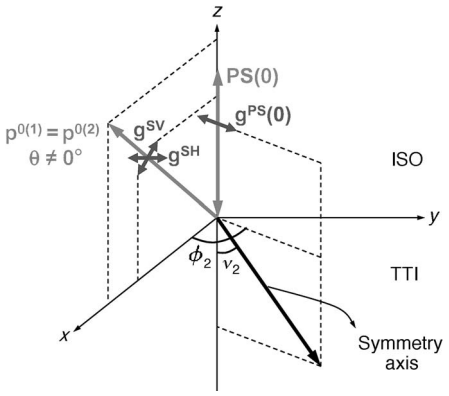

Figure 2. For an isotropic incidence half-space overlying a TTI reflecting half-space, the PS-wave at normal incidence is polarized [vector $\mathbf{g}^{\mathbf{PS}}(\mathbf{0})$] in the symmetry-axis plane of the reflecting half-space. For oblique incidence, we analyze the two components of the PS-wave (PSV and PSH) separately.

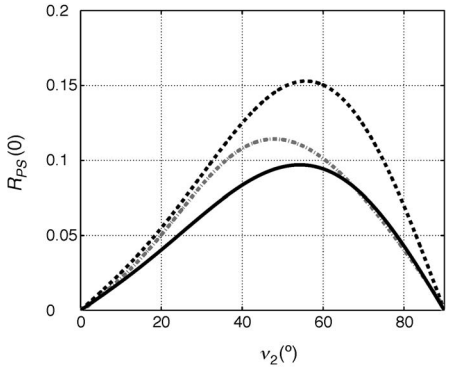

Figure 3. Accuracy of the approximate solutions for the normal-incidence PS-wave reflection coefficient at an isotropic-over-TTI interface. The solid black line is the exact coefficient, the dash-dotted gray line is computed from equation 13 with the exact first derivative of the P-wave phase velocity, and the dashed black line is the fully linearized approximation 12. The tilt ν_2 of the symmetry axis varies from 0° (VTI) to 90° (HTI). The other model parameters are listed in Table 1 [the value of ϕ_2 does not influence $R_{PS}(0)$].

NORMAL-INCIDENCE REFLECTION COEFFICIENT

The normal-incidence reflection coefficient is also called the *intercept* in AVO analysis. The general linearized equation for small-angle PS-wave reflection coefficients can be written as (Jílek, 2002b; Thomsen, 2002)

$$R_{PS} = R_{PS}(0) + G\sin\theta, \qquad (11)$$

where $R_{PS}(0)$ is the normal-incidence reflection coefficient and G is the AVO gradient. In this section, we discuss the dependence of $R_{PS}(0)$ on the parameters of TTI media.

Isotropic-over-TTI interface

First, consider an incidence isotropic half-space overlying a reflecting TTI half-space. The normal-incidence PS-wave in this case is polarized in the symmetry-axis plane of the reflecting half-space (Figure 2). In general, the reflected PS-wave can be represented as the vector sum of the PSV- and PSH-waves. For normal incidence, however, the incidence plane is undefined, and the PS-wave can be studied as a whole. We describe transverse isotropy by the tilt ν and azimuth ϕ of the symmetry axis, the symmetry-direction velocities of the P- and S-waves (V_{P0} and V_{S0}), and the Thomsen anisotropy parameters ϵ, δ, and γ defined with respect to the symmetry axis (Tsvankin, 2005).

The linearized PS-wave normal-incidence reflection coefficient is given by

$$R_{PS}(0) = \frac{g^2\sin 2\nu_2[\cos 2\nu_2(\delta_2 - \epsilon_2) + \epsilon_2]}{4(1+g)} \qquad (12)$$

$$= \frac{g^2}{4(1+g)}\frac{1}{V_{P0,2}}\left.\frac{dV_{P,2}(\xi)}{d\xi}\right|_{\xi=\nu_2}, \qquad (13)$$

where the subscript 2 corresponds to the reflecting half-space and $V_{P,2}(\xi)$ is the P-wave phase velocity in the reflecting half-space as a function of the phase angle ξ with the symmetry axis. It is interesting that the normal-incidence PS-wave reflection coefficient is proportional to the first derivative of the P-wave phase velocity computed at normal incidence ($\xi = \nu_2$). Although this derivative is supposed to be linearized to make equation 13 equivalent to equation 12, the accuracy of the weak-contrast, weak-anisotropy approximation can be increased by using the exact value of this derivative in equation 13 (Figure 3). The model parameters used in Figure 3 and the following figures are given in Table 1.

As expected, equation 12 deteriorates with increasing absolute values of the anisotropy parameters (Figure 4a). The linearized $R_{PS}(0)$ is close to the exact value for models approaching VTI and HTI that have weak PS reflectivity, but the accuracy of the approximations decreases for models with intermediate tilts ν (Figures 3 and 4a). Numerical testing also shows that equations 12 and 13 deviate from the exact solution with the increasing P-to-S velocity ratio in the background $g \equiv \alpha/\beta$ and may become inadequate for soft rocks, such as underwater sediments. On the whole, however, the linearized expressions correctly reproduce the behavior of the normal-incidence reflection coefficient for typical moderately anisotropic TTI models.

The very existence of the normal-incidence PS reflection is caused by the tilt of the symmetry axis away from the vertical and

horizontal directions. Therefore, $R_{PS}(0)$ goes to zero for both a VTI ($\nu_2 = 0°$) medium and an HTI ($\nu_2 = 90°$) medium; the dependence on ν_2 may have minima and maxima at intermediate tilts (Figure 4). For the model in Figure 4a, $R_{PS}(0)$ attains values as high as 0.1 for $\epsilon_2 = 0.3$; in general, the magnitude of $R_{PS}(0)$ increases with ϵ_2.

The dependence of the reflection coefficient on the parameter δ_2 is more complicated (Figure 4b). Apart from the anisotropy parameters, the normal-incidence reflection coefficient also increases with the velocity ratio g.

The coefficient $R_{PS}(0)$ is independent of the parameter γ_2 because the P-wave at normal incidence does not excite SH-waves (governed by γ_2) in the reflecting medium. The variation of $R_{PS}(0)$ with the parameters ϵ_2, δ_2, and ν_2 in Figure 4 can be explained using approximation 12. The influence of ϵ_2 and δ_2 on $R_{PS}(0)$ depends strongly on the tilt ν_2 of the symmetry axis (Figure 5). If the function of ν_2 multiplied with ϵ_2 and δ_2 becomes zero, the corresponding anisotropy parameter makes no contribution to $R_{PS}(0)$. For example, according to approximation 12, δ_2 should have no influence on $R_{PS}(0)$ at $\nu_2 = 45°$. This result is generally supported by the computations of the exact reflection coefficient in Figure 4b, although the curves corresponding to different δ_2 values do not intersect at exactly the same point.

For small tilts ν_2, δ_2 has a greater influence on $R_{PS}(0)$ than does ϵ_2, whereas for larger ν_2 values, the opposite is true. This dependence of $R_{PS}(0)$ on the anisotropy parameters is explained by the behavior of the P-wave phase-velocity function in TI media. At small angles with the symmetry axis, the P-wave velocity in equation 13 is controlled by δ_2, whereas the contribution of ϵ_2 increases toward the isotropy plane (Thomsen, 1986; Tsvankin, 2005).

TTI-over-TTI interface

Next, we consider the normal-incidence PS reflection for a model in which the incidence half-space also is tilted TI. When the incidence medium is anisotropic, the PS reflection splits into the PS_1 and PS_2 modes, which have different normal-incidence reflection coefficients [$R_{PS_1}(0)$ and $R_{PS_2}(0)$] and AVO gradients. According to our convention, the polarization vector of the PS_1-wave lies in the plane formed by the slowness vector and the symmetry axis (i.e., it would be the SV mode if the symmetry axis were vertical). The polarization vector of the PS_2-wave is perpendicular to that plane (i.e., it is the SH mode) (Figure 6). Note that generally the PS_1-wave is not polarized in the horizontal plane, so it is not a "pure" shear mode in terms of its polarization. To explain the influence of the parameters of both half-spaces on the reflection coefficients, we study the linearized approximations for $R_{PS_1}(0)$ and $R_{PS_2}(0)$.

Another complication caused by tilted transverse isotropy in the incidence medium is that the waves PS_1 and PS_2 with vertical slowness vectors (the normal-incidence reflections) are no longer recorded at zero offset. As follows from the results of Tsvankin and Grechka (2002) and Tsvankin (2005), the normal-incidence PS-wave reflection coefficient corresponds to the offset of the PS traveltime minimum in common-midpoint (CMP) geometry. Consequently, the slowness vectors of the zero-offset PS reflections are not vertical. Although the analysis below focuses primarily on the normal-incidence reflections corresponding to the vertical slowness vector, we also give a comparison of the two reflection coefficients for a typical TTI medium.

Model with aligned symmetry planes

If the azimuth of the symmetry axis is the same above and below the reflector (i.e., if $\phi_1 = \phi_2$), the vertical plane that contains both symmetry axes represents a plane of symmetry for the whole model. In this case, the P-wave at normal incidence (i.e., with a vertical slowness vector) excites only one (PS_1) wave polarized in the symmetry-axis plane:

$$R_{PS_1}(0) = \frac{g^2}{4(1+g)}\{-\sin 2\nu_1[\cos 2\nu_1(\delta_1 - \epsilon_1) + \epsilon_1] + \sin 2\nu_2[\cos 2\nu_2(\delta_2 - \epsilon_2) + \epsilon_2]\} \quad (14)$$

Table 1. Medium parameters used in the numerical tests. For all models, the symmetry-direction velocities and densities in the incidence half-space are $V_{P0,1}$ = 2.9 km/s, $V_{S0,1}$ = 1.5 km/s, and ρ_1 = 2.0 g/cm³; in the reflecting half-space, $V_{P0,2}$ = 3.3 km/s, $V_{S0,2}$ = 1.8 km/s, and ρ_2 = 2.2 g/cm³. For isotropic half-spaces, the P- and S-wave velocities are defined by V_{P0} and V_{S0}, respectively. The parameters not listed in the table are specified on the plots.

Figure number	Interface type	Incidence half-space					Reflecting half-space				
		ϵ_1	δ_1	γ_1	ν_1	ϕ_1	ϵ_2	δ_2	γ_2	ν_2	ϕ_2
3	ISO/TTI	0	0	0	–	–	0.4	0.2	0.11		
7	TTI/VTI	0.3	0.1	0.1			0.3	0.15	0.11	0°	–
8	TTI/TTI	0.2	–0.1	0.1	60°		0.2	–0.1	0.1	60°	
9	ISO/TTI	0	0	0	–	–	0.3	0.15	0.11	60°	
10a	TTI/TTI				60°	60°	0.3	0.15	0.11	30°	30°
10b	TTI/TTI	0.2	0.1	0.1	60°	60°				30°	30°
11a and b	TTI/TTI	Same as in Figure 10a and b									
12	TTI/TTI	0.2	0.1	0.1	60°		0.3	0.15	0.11	30°	30°
13	TTI/TTI	Except for ϕ_2, same as in Figure 12									

$$= \frac{g^2}{4(1+g)}\left[- \frac{1}{V_{P0,1}} \left.\frac{dV_{P,1}(\xi)}{d\xi}\right|_{\xi=\nu_1} + \frac{1}{V_{P0,2}} \left.\frac{dV_{P,2}(\xi)}{d\xi}\right|_{\xi=\nu_2}\right], \quad (15)$$

and

$$R_{PS_2}(0) = 0. \quad (16)$$

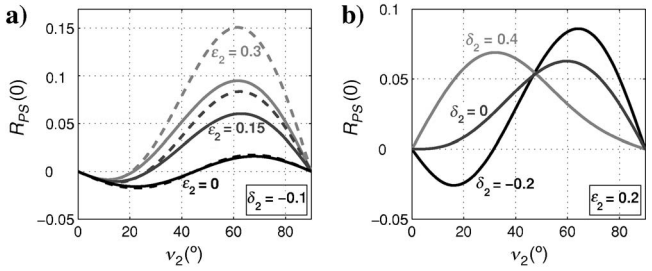

Figure 4. Dependence of the normal-incidence PS-wave reflection coefficient for an isotropic-over-TTI interface on the parameters (a) ϵ_2 and (b) δ_2. The solid lines mark the exact $R_{PS}(0)$, and the dashed lines on plot (a) represent the linearized approximation 12. The densities and symmetry-direction velocities are listed in the title for Table 1.

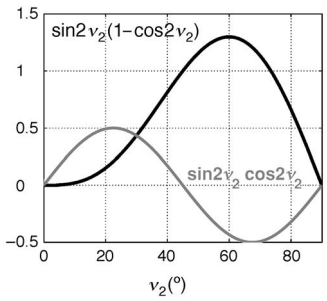

Figure 5. Functions of ν_2 multiplied with ϵ_2 (black line) and δ_2 (gray line) in equation 12. These curves help to explain the influence of ϵ_2 and δ_2 on $R_{PS}(0)$ for different tilts ν_2 in Figures 4a and b.

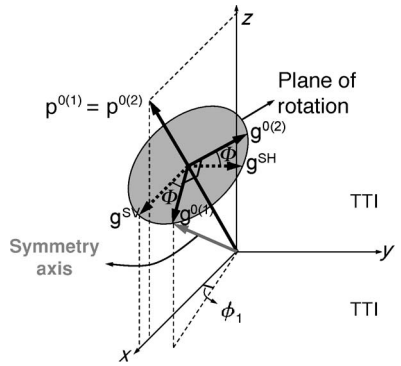

Figure 6. For an incidence TI half-space, the polarization vector $\mathbf{g}^{0(1)}$ of the PS_1-wave lies in the plane formed by the slowness vector and the symmetry axis (i.e., it would correspond to the SV-wave, if the symmetry axis were vertical). The vector $\mathbf{g}^{0(2)}$ of the PS_2-wave is perpendicular to that plane (SH-wave).

In keeping with the symmetry of the problem, the coefficient $R_{PS_1}(0)$ vanishes when both half-spaces are either VTI or HTI, and $\sin 2\nu_1 = \sin 2\nu_2 = 0$. $R_{PS_1}(0)$ is a function of both tilts (ν_1 and ν_2) and all anisotropy parameters except for γ_1 and γ_2 — the parameters responsible for SH-wave propagation in TI media.

The term involving ν_1, ϵ_1, and δ_1 in equation 14 has the same form (but the opposite sign) as that involving ν_2, ϵ_2, and δ_2. Thus the conclusions drawn above for the influence of ν_2, ϵ_2, and δ_2 (Figure 5) apply to ν_1, ϵ_1, and δ_1 as well. If both TI half-spaces have the same orientation of symmetry axes and the same parameters ϵ and δ, $R_{PS_1}(0)$ vanishes, even though there may be a jump in the other parameters across the interface. Although this result is strictly valid only in the weak-contrast, weak-anisotropy limit, the exact coefficient $R_{PS_1}(0)$ for models with $\nu_1 = \nu_2$, $\phi_1 = \phi_2$, $\epsilon_1 = \epsilon_2$, and $\delta_1 = \delta_2$ is quite small (see below).

As mentioned above, if the incidence half-space is anisotropic, the normal-incidence PS-wave reflection coefficient discussed here may be different from the reflection coefficient at zero offset (Figure 7). However, when the incidence medium is VTI or HTI, these two coefficients are identical. For a tilt of $\nu_1 = 50°$ in Figure 7, the zero-offset reflection coefficient of the PS_1-wave is almost 40% larger by absolute value than the normal-incidence coefficient that determines the reflection amplitude at the traveltime minimum in a CMP gather.

General TTI-over-TTI model

If the symmetry axis has different azimuths above and below the reflector, then a P-wave at normal incidence excites both PS modes. The approximate solutions for the reflection coefficients $R_{PS_1}(0)$ and $R_{PS_2}(0)$ are

$$R_{PS_1}(0) = \frac{g^2}{4(1+g)}\{-\sin 2\nu_1[\cos 2\nu_1(\delta_1 - \epsilon_1) + \epsilon_1] + \cos(\phi_2 - \phi_1)\sin 2\nu_2[\cos 2\nu_2(\delta_2 - \epsilon_2) + \epsilon_2]\} \quad (17)$$

$$= \frac{g^2}{4(1+g)}\left[- \frac{1}{V_{P0,1}} \left.\frac{dV_{P,1}(\xi)}{d\xi}\right|_{\xi=\nu_1} + \cos(\phi_2 - \phi_1)\frac{1}{V_{P0,2}} \left.\frac{dV_{P,2}(\xi)}{d\xi}\right|_{\xi=\nu_2}\right], \quad (18)$$

$$R_{PS_2}(0) = \frac{g^2}{4(1+g)}\{\sin(\phi_2 - \phi_1)\sin 2\nu_2[\cos 2\nu_2(\delta_2 - \epsilon_2) + \epsilon_2]\} \quad (19)$$

$$= \frac{g^2}{4(1+g)} \sin(\phi_2 - \phi_1)\frac{1}{V_{P0,2}} \left.\frac{dV_{P,2}(\xi)}{d\xi}\right|_{\xi=\nu_2}. \quad (20)$$

It is clear from the symmetry of the model (TTI-over-TTI) that the normal-incidence reflection coefficients should depend just on the difference $\phi_2 - \phi_1$, which is confirmed by equations 17–20. Indeed, a simultaneous azimuthal rotation of both symmetry axes can change only the azimuthal direction of the polarization vectors of the PS-waves. When the vertical-symmetry planes of the two TI half-

spaces coincide (when $\phi_1 = \phi_2$), equations 17 and 18 reduce to equations 14 and 15, respectively, and $R_{PS_2}(0) = 0$.

Despite the relative azimuthal rotation of the symmetry axes, the terms involving the tilt of the symmetry axis and the anisotropy parameters in equations 17 and 19 keep the same form as the corresponding terms for the simpler isotropic-over-TTI model examined above. Both linearized reflection coefficients are governed just by the velocity ratio g, the azimuthal angle between the symmetry axes, and the derivatives of the P-wave phase velocity. This result is particularly surprising for the PS_2-wave (the SH-wave) whose velocity after the reflection is controlled by the parameter γ_1, which does not contribute at all to the coefficient $R_{PS_2}(0)$. The absence of the γ parameters in equations 17 and 19 can be explained by the independence of the stiffness coefficients c_{34} and c_{35} [which are responsible for $R_{PS}(0)$] from both γ_1 and γ_2. It also is noteworthy that the parameters of the reflecting half-space do not contribute to $R_{PS_1}(0)$ when the symmetry axes lie in orthogonal planes (i.e., $|\phi_1 - \phi_2| = 90°$).

As we discussed above, if both TI half-spaces have the same P-wave phase-velocity functions (i.e., the same parameters ϕ, ν, ϵ, and δ), the linearized $R_{PS_1}(0)$ and $R_{PS_2}(0)$ (equations 17–20) go to zero. Figure 8 confirms that the exact coefficient $R_{PS_2}(0)$ in this case ($\phi_1 = \phi_2$) is indeed insignificant (although not exactly zero). On the other hand, if the symmetry axes are tilted in opposite directions from the vertical (i.e., if $\nu_1 = \nu_2$, but $\phi_1 - \phi_2 = 180°$), the normal-incidence reflection coefficient may exceed 0.1 even for moderately anisotropic models (Figure 8).

AVO GRADIENTS

The AVO gradients of the split PS-waves can be computed numerically by estimating the best-fit initial slope of the exact reflection coefficient expressed as a function of $\sin\theta$. In the linearized weak-anisotropy, weak-contrast approximation, the gradient G is obtained explicitly as the multiplier of $\sin\theta$ (equation 11). The approximate AVO gradients of the waves PS_1 and PS_2 are given in Appendix B.

Isotropic-over-TTI interface

If the incidence medium is isotropic, wave PS_1 becomes an SV mode polarized in the incidence plane, and wave PS_2 represents an SH-wave. Because there is no P-to-SH conversion in isotropic media, the gradient $G_{PS_2} = G_{PSH}$ is purely anisotropic, although $G_{PS_1} = G_{PSV}$ contains both isotropic and anisotropic terms (equations B-1 and B-2).

In the linearized approximation, the reflection coefficients for isotropic media coincide with the isotropic terms in the coefficients for the isotropic-over-TTI interface (Appendix B). For example, the expression for G_{PSV} reduces to the familiar gradient for isotropic media (e.g., Nefedkina and Buzlukov, 1999), if $\epsilon_2 = \delta_2 = \gamma_2 = 0$. Numerical testing shows that for common values of the velocity ratio g, the AVO gradients are not distorted significantly by the anisotropy (Figure 9). The influence of the anisotropy in the reflecting half-space primarily changes the normal-incidence coefficient $R_{PS}(0)$, which goes to zero in the isotropic model. Although the AVO gradients of both PS-waves vary with azimuth, their average values are close to those for isotropic media, and the magnitude of the azimuthal variations is relatively insignificant. In particular, gradient G_{PSH} is small, and the reflection coefficient of the PSH-wave is almost constant (Figure 9).

Because the dependence of the AVO gradients on the Thomsen parameters of the reflecting medium is rather complicated, in partic-

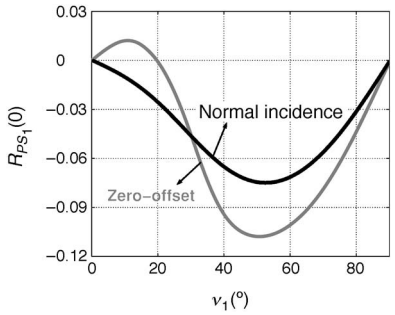

Figure 7. Comparison of the exact normal-incidence (black curve) and the zero-offset (gray curve) PS_1-wave reflection coefficients for a TTI-over-VTI interface. The normal-incidence coefficient is computed for a vertical slowness vector of the incident wave and would be recorded at nonzero offset. The model parameters are listed in Table 1 (the value of ϕ_1 does not influence the results).

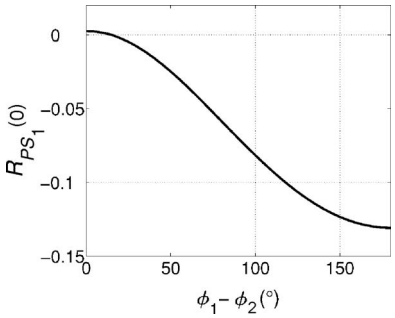

Figure 8. Exact $R_{PS_1}(0)$ for a TTI-over-TTI interface as a function of the difference between the azimuths of the symmetry axes. The tilt ν and anisotropy parameters ϵ, δ, and γ (listed in Table 1) are the same in both half-spaces. Note that the tilt is measured from the vertical toward the radius vector oriented at an azimuth ϕ.

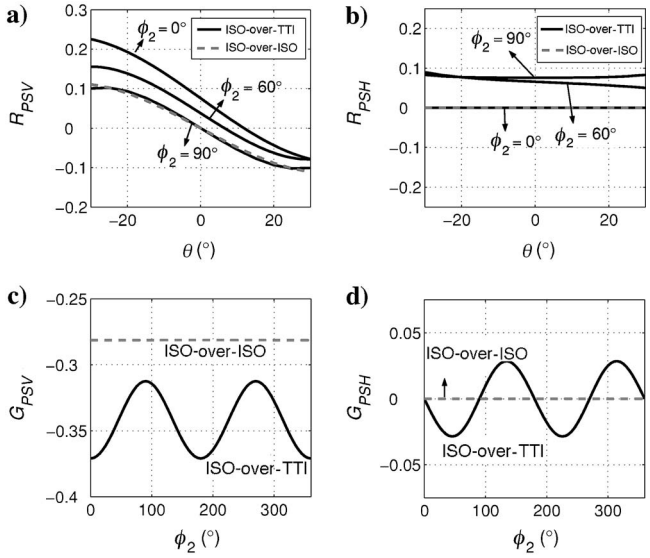

Figure 9. Exact PS-wave reflection coefficients (top row) and AVO gradients (bottom row) for isotropic-over-isotropic and isotropic-over-TTI interfaces (Table 1).

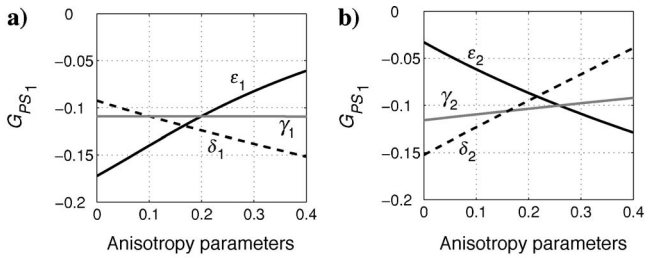

Figure 10. Exact AVO gradient of the PS_1-wave for a TTI-over-TTI interface (Table 1), as a function of the anisotropy parameters in the (a) incidence and (b) reflecting half-spaces.

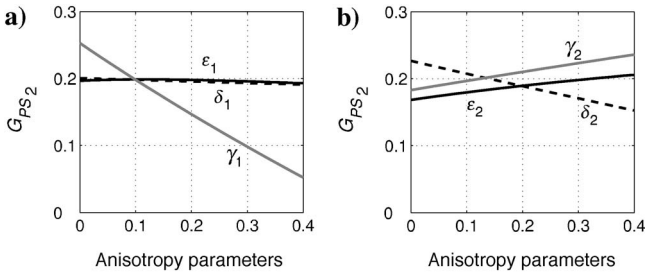

Figure 11. Exact AVO gradient of the PS_2-wave for a TTI-over-TTI interface as a function of the anisotropy parameters in the (a) incidence and (b) reflecting half-spaces. The model parameters are the same as in Figure 10.

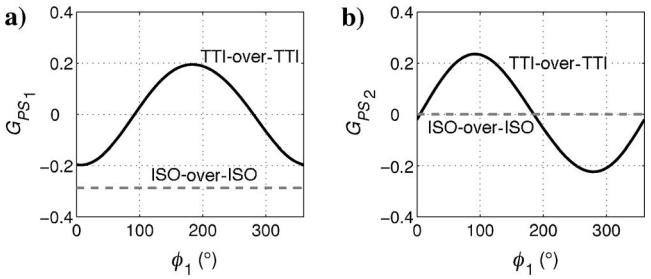

Figure 12. Exact AVO gradients of the (a) PS_1-waves and (b) the PS_2-waves as functions of the azimuth ϕ_1 for TTI-over-TTI (solid line) and isotropic-over-isotropic (dashed) interfaces. The parameters of the TTI-over-TTI model are listed in Table 1. As before, the isotropic model is defined by the symmetry-direction velocities and densities used for the TTI-over-TTI interface.

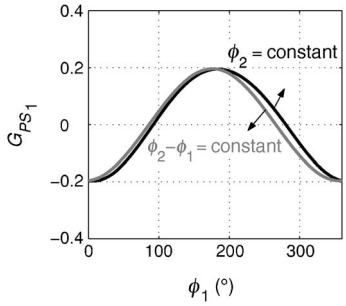

Figure 13. Exact PS_1-wave AVO gradient as a function of the azimuth ϕ_1 for a TTI-over-TTI interface. The black line corresponds to $\phi_2 = 30°$ and the gray line to $\phi_2 - \phi_1 = 30°$. The other model parameters are the same as those for the TTI-over-TTI model in Figure 12.

ular for the PSV-wave (equation B-1), we studied the behavior of the exact gradients using numerical modeling. As was the case for $R_{PS}(0)$, the influence of ϵ_2 on both G_{PSV} and G_{PSH} increases with the tilt ν_2, whereas the influence of δ_2 on those parameters decreases with the tilt. In contrast to the normal-incidence reflection coefficients, both AVO gradients depend on parameter γ_2, and the contribution of γ_2 grows with ν_2.

The gradient G_{PSH} goes to zero when the symmetry axis lies in the incidence plane and there is no P-to-SH conversion (Figure 9, $\phi_2 = 0°$) or when the symmetry axis lies in the plane orthogonal to the acquisition line ($\phi_2 = 90°$). Because the PSH-wave vanishes for a reflecting VTI half-space, the gradient G_{PSH} increases with ν_2 as the symmetry axis deviates from the vertical direction.

TTI-over-TTI interface

Because of the limitations related to the contribution of the polarization angle Φ (see above), the AVO gradients of the PS_1- and PS_2-waves for a TTI-over-TTI interface were derived only for two special cases (see Appendix B). The symmetry axis of the incidence half-space was assumed to be confined either to the incidence plane (equations B-3 and B-4) or to the horizontal plane (HTI medium; equations B-5 and B-6). We also present numerical results for an arbitrary orientation of the symmetry axis of the incidence medium.

As Figures 10 and 11 illustrate, the two AVO gradients are sensitive to different anisotropy parameters of the incidence medium. Whereas the gradient G_{PS_1} is controlled by ϵ_1 and δ_1 (Figure 10), G_{PS_2} depends only on γ_1 (Figure 11). To explain this result for an arbitrary orientation of the symmetry axis of the incidence half-space, note that the velocity of the S_1-wave is a function of ϵ_1 and δ_1 (S_1 would become SV in VTI media). In contrast, the only anisotropy parameter responsible for the velocity of the S_2-wave is γ_1 (S_2 would become SH in VTI media).

If the incidence half-space is TTI and the symmetry axis is not confined to the incidence plane, there are no purely isotropic terms in either gradient, as equations B-5 and B-6 demonstrate for the special case of the HTI incidence medium. The influence of the anisotropy in the upper half-space causes the gradients computed for a TTI-over-TTI interface to deviate substantially from those for the corresponding isotropic model (compare Figures 12 and 9). The azimuthal variation of both gradients also is much more pronounced than that for the isotropic-over-TTI interface. The relatively small contribution that the anisotropy of the reflecting half-space makes to the AVO gradients is evident in Figure 13, where G_{PS_1} is weakly dependent on the symmetry-axis azimuth ϕ_2.

CONCLUSIONS

In the absence of lateral heterogeneity, anisotropy is the most likely reason for significant PS-wave energy at small offsets observed in many multicomponent data sets. Here, we analyze the small-angle PS-wave AVO response for transverse isotropy with a tilted symmetry axis (i.e., for a TTI medium). Unless the reflector coincides with a symmetry plane in both half-spaces, a P-wave at normal incidence always generates reflected PS-waves. To examine the influence of the anisotropy parameters on the normal-incidence PS-wave reflection coefficient and AVO gradient, we employ linearized solutions (weak-contrast, weak-anisotropy approximations) supported by numerical modeling of the exact reflection coefficient.

If the incidence half-space is isotropic, the PS reflection from a horizontal interface is polarized in the symmetry-axis plane of the

reflecting TTI medium. The normal-incidence reflection coefficient $R_{PS}(0)$ vanishes when the reflecting TI half-space is VTI or HTI, because in that case the model as a whole has a horizontal symmetry plane. The coefficient $R_{PS}(0)$ increases rapidly as the symmetry axis deviates from both the vertical and horizontal directions. Closed-form approximations and numerical modeling show that $R_{PS}(0)$ can be as large as 0.1, even for moderate values of the anisotropy parameters such as those typical for shale formations. When the tilt ν_2 of the symmetry axis is relatively small, the coefficient $R_{PS}(0)$ is controlled mostly by the parameter δ_2 (the Thomsen parameter δ in the reflecting half-space), the contribution of ϵ_2 becoming dominant for larger values of ν_2.

When both half-spaces are anisotropic (TTI), a P-wave at normal incidence excites two split PS-waves (PS_1 and PS_2) with polarizations governed by the orientation of the symmetry axis in the incidence medium. The normal-incidence reflection coefficients of both PS-waves [$R_{PS_1}(0)$ and $R_{PS_2}(0)$] are functions of the difference between the azimuths of the symmetry axes ($\phi_2 - \phi_1$) and do not depend on either azimuth individually. Interestingly, the Thomsen parameters and the tilt of the symmetry axis in both half-spaces contribute to the linearized coefficients $R_{PS_1}(0)$ and $R_{PS_2}(0)$, but that contribution is completely absorbed by the first derivative of the P-wave phase-velocity function. The coefficients $R_{PS_1}(0)$ and $R_{PS_2}(0)$ are insignificant when the two half-spaces have the same symmetry-axis orientation and the same parameters ϵ and δ, even though there may be a jump in the velocities and densities across the interface.

We also discussed the azimuthally varying AVO gradients of PS-waves at small incidence angles. The gradients are influenced primarily by the incidence medium's anisotropy, which causes shear-wave splitting and pronounced azimuthal variation of the reflection coefficients of both PS modes. For an arbitrary symmetry-axis orientation, neither linearized AVO gradient contains purely isotropic terms because the contributions of the velocity and density contrasts are multiplied with functions of the symmetry-axis azimuth ϕ_1.

The linearized approximations we developed here not only provide physical insight into the behavior of the PS-wave reflection coefficients but also can be used to quickly evaluate PS-wave amplitudes for a wide range of TTI models. Potentially, these analytic expressions can help in the AVO inversion of PP and PS data for TTI media.

ACKNOWLEDGMENTS

We are grateful to members of the A(nisotropy)-Team of the Center for Wave Phenomena (CWP), Colorado School of Mines and P. Jílek (BP Americas) for helpful discussions. We thank Mike Mueller of BP for drawing our attention to the presence of small-offset PS-wave energy in field records. The support for this work was provided by the Consortium Project on Seismic Inverse Methods for Complex Structures at CWP and by the Chemical Sciences, Geosciences and Biosciences Division, Office of Basic Energy Sciences, U.S. Department of Energy.

APPENDIX A

PERTURBATION APPROACH FOR THE REFLECTION/TRANSMISSION PROBLEM

The approximate linearized reflection and transmission coefficients are derived by using an isotropic full space as the reference medium. A horizontal planar interface (reflector) divides the full space into two half-spaces, which are perturbed to obtain two weakly anisotropic media:

$$a^{(I)}_{ijkl} = a^0_{ijkl} + \delta a^{(I)}_{ijkl}, \tag{A-1}$$

$$\rho^{(I)} = \rho^0 + \delta\rho^{(I)}, \tag{A-2}$$

$$|\delta a^{(I)}_{ijkl}| \ll \|a^0_{ijkl}\|, \tag{A-3}$$

$$|\delta\rho^{(I)}| \ll \rho^0. \tag{A-4}$$

In equation A-4, the index I ($I = 1,2$) stands for the incidence and reflecting half-spaces, respectively, and a^0_{ijkl} and ρ^0 are the density-normalized stiffness coefficients and density of the background isotropic medium. Because the perturbations from the isotropic background in both half-spaces are small, the approximation involves both weak anisotropy and weak elastic contrast between the half-spaces. Using these approximations, the polarization vector ($\mathbf{p}^{(N)}$) and the slowness vector ($\mathbf{g}^{(N)}$) can be linearized as.

$$\begin{aligned}\mathbf{g}^{(N)} &\approx \mathbf{g}^{0(N)} + \delta\mathbf{g}^{(N)},\\ \mathbf{p}^{(N)} &\approx \mathbf{p}^{0(N)} + \delta\mathbf{p}^{(N)},\end{aligned} \tag{A-5}$$

where $\mathbf{p}^{0(N)}$ and $\mathbf{g}^{0(N)}$ are the polarization vector and the slowness vector, respectively, of waves propagating in the background isotropic medium, and $\delta\mathbf{g}^{(N)}$ and $\delta\mathbf{p}^{(N)}$ are their linear perturbations. Analytic expressions for the perturbations $\delta\mathbf{g}^{(N)}$ and $\delta\mathbf{p}^{(N)}$ in terms of $\delta a^{(I)}_{ijkl}$ are given in Vavryčuk and Pšenčík (1998) and Jílek (2002b). Substituting these linearized expressions into equation 1 of the main text yields

$$(\mathbf{C^0} + \delta\mathbf{C})(\mathbf{U^0} + \delta\mathbf{U}) = \mathbf{B^0} + \delta\mathbf{B}. \tag{A-6}$$

Here, $\mathbf{C^0}$ is the stiffness matrix of the background medium and $\delta\mathbf{U}$ is the perturbation of the reflection and transmission coefficients in the background isotropic medium ($\mathbf{U^0}$). Because the background is homogeneous, $\mathbf{U^0}$ is given by

$$\mathbf{U^0} = [0,\ 0,\ 0,\ 0,\ 0,\ 1]^{\mathbf{T}}. \tag{A-7}$$

Expanding equation A-6 and retaining only the leading terms in small quantities results in the equation

$$\delta\mathbf{U} = (\mathbf{C^0})^{-1}(\delta\mathbf{B} - \delta\mathbf{C}\cdot\mathbf{U^0}), \tag{A-8}$$

where

$$\delta\mathbf{C} = \begin{bmatrix} \delta g_1^{(1)} & \delta g_1^{(2)} & \delta g_1^{(3)} & -\delta g_1^{(4)} & -\delta g_1^{(5)} & -\delta g_1^{(6)} \\ \delta g_2^{(1)} & \delta g_2^{(2)} & \delta g_2^{(3)} & -\delta g_2^{(4)} & -\delta g_2^{(5)} & -\delta g_2^{(6)} \\ \delta g_3^{(1)} & \delta g_3^{(2)} & \delta g_3^{(3)} & -\delta g_3^{(4)} & -\delta g_3^{(5)} & -\delta g_3^{(6)} \\ \delta X_1^{(1)} & \delta X_1^{(2)} & \delta X_1^{(3)} & -\delta X_1^{(4)} & -\delta X_1^{(5)} & -\delta X_1^{(6)} \\ \delta X_2^{(1)} & \delta X_2^{(2)} & \delta X_2^{(3)} & -\delta X_2^{(4)} & -\delta X_2^{(5)} & -\delta X_2^{(6)} \\ \delta X_3^{(1)} & \delta X_3^{(2)} & \delta X_3^{(3)} & -\delta X_3^{(4)} & -\delta X_3^{(5)} & -\delta X_3^{(6)} \end{bmatrix}, \tag{A-9}$$

$$\delta\mathbf{B} = -[\delta g_1^{(0)},\ \delta g_2^{(0)},\ \delta g_3^{(0)},\ \delta X_1^{(0)},\ \delta X_2^{(0)},\ \delta X_3^{(0)}]^{\mathbf{T}}. \tag{A-10}$$

Therefore, the perturbed vector of the reflection-over-transmission coefficients is obtained as

$$\delta\mathbf{U} = (\mathbf{C^0})^{-1}[\delta g_1^{(6)} - \delta g_1^{(0)},\ \delta g_2^{(6)} - \delta g_2^{(0)},\ \delta g_3^{(6)} - \delta g_3^{(0)},\ \delta X_1^{(6)} - \delta X_1^{(0)},\ \delta X_2^{(6)} - \delta X_2^{(0)},\ \delta X_3^{(6)} - \delta X_3^{(0)}]. \quad \text{(A-11)}$$

APPENDIX B

APPROXIMATE PS-WAVE AVO GRADIENTS IN TI MEDIA

Here, we present linearized expressions for the AVO gradients of the PS_1- and PS_2-waves (G_{PS_1} and G_{PS_2}) obtained in the weak-contrast, weak-anisotropy limit. If the incidence half-space is isotropic, the PS_1-wave becomes a PSV mode with in-plane polarization, and PS_2 becomes a transversely polarized PSH-wave. The gradients for these waves have the form

$$G_{PSV} = G_{PS_1} = -\frac{2\Delta V_{S0}}{g\beta} - \frac{(2+g)\Delta\rho}{2g\rho^0} - \frac{2\gamma_2 \sin^2\nu_2 \sin^2\phi_2}{g} + \frac{g}{16(1+g)}\{(3+2g)\delta_2 + (3-2g)(\delta_2-\epsilon_2)\cos 4\nu_2 - (1+2g)\epsilon_2 + 2\cos 2\nu_2[\delta_2 + 2(-1+2g)(\delta_2-\epsilon_2) \times \cos 2\phi_2 \sin^2\nu_2 + 2\epsilon_2] + 4(2g\delta_2 - \epsilon_2 - 2g\epsilon_2) \times \cos 2\phi_2 \sin^2\nu_2\}, \quad \text{(B-1)}$$

$$G_{PSH} = G_{PS_2} = \frac{\gamma_2 \sin^2\nu_2 \sin 2\phi_2}{g} + \frac{g \sin^2\nu_2 \sin 2\phi_2}{4(1+g)}\{(\delta_2-\epsilon_2) \times [2g + (-1+2g)\cos 2\nu_2] - \epsilon_2\}. \quad \text{(B-2)}$$

The AVO gradients for a TTI-over-TTI interface are given here for only two special cases. If the incidence plane contains the symmetry axis of the incidence TTI half-space ($\phi_1 = 0°$), the gradients are given by

$$G_{PS_1} = -\frac{2\Delta V_{S0}}{g\beta} - \frac{(2+g)\Delta\rho}{2g\rho^0} - \frac{2\gamma_2 \sin^2\nu_2 \sin^2\phi_2}{g} + \frac{g}{16(1+g)}\{-4(1+g)(\delta_1-\epsilon_1) + 4(-1+g) \times(\delta_1-\epsilon_1)\cos 4\nu_1 - 8\epsilon_1\cos 2\nu_1 + 3\delta_2 - \epsilon_2 + 2g(\delta_2-\epsilon_2) + 2(\delta_2+2\epsilon_2)\cos 2\nu_2 + 4\cos 2\phi_2 \sin^2\nu_2\{(\delta_2-\epsilon_2)[2g + (-1 + 2g)\cos 2\nu_2] - \epsilon_2\} + (3-2g)(\delta_2-\epsilon_2)\cos 4\nu_2\}, \quad \text{(B-3)}$$

$$G_{PS_2} = \frac{\gamma_2 \sin^2\nu_2 \sin 2\phi_2}{g} + \frac{g \sin^2\nu_2 \sin 2\phi_2}{4(1+g)}\{(\delta_2-\epsilon_2) \times [2g + (-1+2g)\cos 2\nu_2] - \epsilon_2\}. \quad \text{(B-4)}$$

If the symmetry axis of the upper half-space deviates from the incidence plane, fully linearized AVO gradients still can be derived for the special case of the incidence HTI medium:

$$G_{PS_1}^{\mathrm{HTI}} = -\frac{2\Delta V_{S0}\cos\phi_1}{g\beta} - \frac{(2+g)\Delta\rho\cos\phi_1}{2g\rho^0} - \frac{2\gamma_2 \sin^2\nu_2 \sin(\phi_2-\phi_1)\sin\phi_2}{g} + \frac{g}{16(1+g)}\{4\sin^2\nu_2\cos(2\phi_2-\phi_1)\{(\delta_2-\epsilon_2) \times [2g + (-1+2g)\cos 2\nu_2] - \epsilon_2\} + \cos\phi_1[-8\delta_1 + 16\epsilon_1 + 3\delta_2 - \epsilon_2 + 2g(\delta_2-\epsilon_2) + 2(\delta_2+2\epsilon_2)\cos 2\nu_2 - (-3+2g) \times (\delta_2-\epsilon_2)\cos 4\nu_2]\}, \quad \text{(B-5)}$$

$$G_{PS_2}^{\mathrm{HTI}} = \frac{2\Delta V_{S0}\sin\phi_1}{g\beta} + \frac{(2+g)\Delta\rho\sin\phi_1}{2g\rho^0} - \frac{2\gamma_1\sin\phi_1}{g} + \frac{2\gamma_2 \sin^2\nu_2 \cos(\phi_2-\phi_1)\sin\phi_2}{g} + \frac{g}{16(1+g)}\{4\sin^2\nu_2\sin(2\phi_2-\phi_1)\{(\delta_2-\epsilon_2) \times [2g + (-1+2g)\cos 2\nu_2] - \epsilon_2\} - \sin\phi_1[3\delta_2 - \epsilon_2 + 2g(\delta_2-\epsilon_2) + 2(\delta_2+2\epsilon_2) \times \cos 2\nu_2 - (-3+2g)(\delta_2-\epsilon_2)\cos 4\nu_2]\}. \quad \text{(B-6)}$$

REFERENCES

Aki, K., and P. G. Richards, 2002, Quantitative seismology, 2nd ed.: University Science Books.

Alvarez, K., M. Donati, and M. Aldana, 1999, AVO analysis for converted waves: 69th Annual International Meeting, SEG, Expanded Abstracts, 876–879.

Angerer, E., S. A. Horne, J. E. Gaiser, R. Walters, S. Bagala, and L. Vetri, 2002, Characterization of dipping fractures using PS mode-converted data: 72nd Annual International Meeting, SEG, Expanded Abstracts, 1010–1013.

Artola, F. A. V., R. Leiderman, and S. A. B. Fontoura, 2005, Zero-offset P-S energy in horizontally layered media: Geophysical Prospecting, **53**, 717–721.

Banik, N. C., 1987, An effective anisotropy parameter in transversely isotropic media: Geophysics, **52**, 1654–1664.

Donati, S. M., 1998, Making AVO analysis for converted waves a practical issue: 68th Annual International Meeting, SEG, Expanded Abstracts, 2060–2063.

Jech, J., and I. Pšenčík, 1989, First-order perturbation method for anisotropic media: Geophysical Journal International, **99**, 369–376.

Jílek, P., 2002a, Converted PS-wave reflection coefficients in weakly anisotropic media: Pure and Applied Geophysics, **159**, 1527–1562.

——, 2002b, Modeling and inversion of converted-wave reflection coefficients in anisotropic media: A tool for quantitative AVO analysis, Ph.D. thesis, Colorado School of Mines.

Larsen, A. J., F. G. Margrave, and H.-X. Lu, 1999, AVO analysis by simultaneous P-P and P-S weighted stacking applied to 3C-3D seismic data: 69th

Annual International Meeting, SEG, Expanded Abstracts, 721–724.
Nefedkina, T., and V. Buzlukov, 1999, Seismic dynamic inversion using multiwave AVO data: 69th Annual International Meeting, SEG, Expanded Abstracts, 888–891.
Pšenčík, I., and V. Vavryčuk, 1998, Weak contrast PP wave displacement R/T coefficients in weakly anisotropic elastic media: Pure and Applied Geophysics, **151**, 699–718.
Rüger, A., 1996, Reflection coefficients and azimuthal AVO analysis in anisotropic media: Ph.D. thesis, Colorado School of Mines.
———, 1998, Variation of P-wave reflectivity with offset and azimuth in anisotropic media: Geophysics, **63**, 935–947.
———, 2001, Reflection coefficients and azimuthal AVO analysis in anisotropic media: SEG.
Shuey, R. T., 1985, A simplification of Zoeppritz equations: Geophysics, **50**, 609–614.
Thomsen, L., 1986, Weak elastic anisotropy: Geophysics, **51**, 1954–1966.
———, 1993, Weak anisotropic reflections, *in* J. P. Castagna and M. M. Backus, eds., Offset dependent reflectivity: SEG.
———, 2002, Understanding seismic anisotropy in exploration and exploitation: Distinguished Instructor Short Course (DISC) 5, SEG and EAGE.
Tsvankin, I., 1995, Seismic wavefields in layered isotropic media: Samizdat Press, Colorado School of Mines.
———, 2005, Seismic signatures and analysis of reflection data in anisotropic media, 2nd ed.: Elsevier Science Publishing Company, Inc.
Tsvankin, I., and V. Grechka, 2002, 3D description and inversion of reflection moveout of PS-waves in anisotropic media: Geophysical Prospecting, **50**, 301–316.
Vavryčuk, V., 1999, Weak-contrast reflection/transmission coefficients in weakly anisotropic elastic media, P-wave incidence: Geophysical Journal International, **138**, 553–562.
Vavryčuk, V., and I. Pšenčík, 1998, PP-wave reflection coefficients in weakly anisotropic elastic media: Geophysics, **63**, 2129–2141.